

# Chapter 11

## Amphiphilic, Thermoresponsive Polymers Interacting with Explicit Solvent



Yukiteru Katsumoto

### Contents

11.1 Introduction: Polymer and Solvent .....	338
11.2 Solvation of Polymers at Molecular Level .....	340
11.3 How the Intramolecular Interactions Affect the Properties of Polymers in Solution ....	348
11.4 Block Design of Amphiphilic Copolymers .....	352
11.5 Conclusion .....	357
References .....	357

**Abstract** The relationship between the solvent molecules and the properties of amphiphilic polymers will be discussed. For representative amphiphilic polymers, we focus on poly(*N,N*-diethylacrylamide) (PNdEAm), poly(*N*-isopropylacrylamide) (PNiPAm), and poly(ethylene oxide) (PEO)-based alternating multiblock (AMB) copolymers, which exhibit thermoresponsive behaviors in water. When the role of solvents in the intra- and intermolecular interaction of solvated polymers is investigated, one encounters several cases that require to consider the solvents as explicit molecules. There are mainly two topics in this chapter: the solvation of synthetic polymers at the molecular level and the hydrophobic interaction of AMB copolymers. The infrared spectroscopy shows how the solvation state of the monomer model compounds and polymers are different at the molecular level. For PNdEAm and PNiPAm in solution, the interaction among the neighboring chains often competes with the solvation of themselves. The phase diagrams of the aqueous solution of the stereocontrolled PNdEAm and PNiPAm clearly reveal that the intramolecular interaction modifies their hydrophilicity. In the last section, the AMB architectures for designing amphiphilic polymers will be introduced, which are expected to form polymer assemblies in water.

---

Y. Katsumoto (✉)

Faculty of Science, Department of Chemistry, Fukuoka University, Jonan-ku, Fukuoka, Japan  
e-mail: [katsumoto@fukuoka-u.ac.jp](mailto:katsumoto@fukuoka-u.ac.jp)

**Keywords** Poly(acrylamide) derivatives · Hydration · Tacticity dependence on the solubility of polymers · Infrared spectroscopy · Alternating multiblock copolymers · Poly(*N*-isopropylacrylamide) · Poly(*N,N*-diethylacrylamide) · *N*-methylacetamide · *N,N*-diethylacetamide · Poly(ethylene oxide) · Amide vibration · Lower critical solution temperature · Phase separation · Phase boundary · Random copolymerization · Aqueous solution · Hydration · Solvation · Tacticity · Infrared Spectroscopy · Amphiphilic polymer · Micellization · Alternating multiblock copolymers

## 11.1 Introduction: Polymer and Solvent

For investigating the fundamental properties of polymers, solvents are always the key factor. Because the characterization of polymers cannot be performed in the gas phase, we should select an appropriate solvent for the target. The unperturbed state of a polymer chain, for example, is found in a specific solvent, which is so-called the theta ( $\theta$ ) solvent [8]. The  $\theta$  temperature is a temperature at which the polymer chains act like as an unperturbed, ideal chain in the  $\theta$  solvent. Under the  $\theta$  condition, the random-walk coil dimensions are expected for polymer chains. Table 11.1 lists several examples for the combinations of a polymer and its  $\theta$  solvent together with the  $\theta$  temperature [1–7]. At the  $\theta$  temperature, the solvent effect is assumed to be omitted in the analysis of the chain conformation and morphology. When the perturbation is not large, the solvent effects can be taken into account as a continuous medium. At the dawn of polymer science, therefore, solvent molecules have not been explicitly treated. In the Flory-Huggins model, for example, the  $\chi$  parameter that implicitly expresses polymer-solvent interactions determines the solubility of the polymer into the solvent [9, 10]. In this framework, the  $\theta$  temperature is interpreted as the temperature at which the polymer-solvent interaction apparently disappears. Even though the solvent effect is described by a single parameter, the Flory-Huggins model succeeds to predict how the polymer solution undergoes a phase separation with the upper critical solution temperature (UCST), where the phase separation occurs by cooling the system. In the UCST

**Table 11.1** The  $\theta$  solvent and temperature for several polymers

Polymer	$\theta$ solvent	$\theta$ temperature/ $^{\circ}$ C
Polyethylene	Diphenyl ether [1]	164
	Diphenyl methane [1]	128
Polystyrene/atactic	Cyclohexane [2]	31
	Trans-decalin [3]	34
Poly(methyl methacrylate)/atactic	Acetonitrile [4]	45
	3-octane [5]	72
Poly(ethylene oxide)	Water [6]	59
Poly( <i>N</i> -isopropylacrylamide)/atactic	Water [7]	31

system, the attractive interaction among polymers overcomes the solvent-polymer attractive interaction as the temperature goes down. The second virial coefficient, which describes the contribution of the pair-wise potential to the osmotic pressure of the polymer solution, vanishes at the  $\theta$  temperature. Here the solvent plays only a minor role as a continuum medium that may strengthen or weaken the interaction among the solutes.

As polymer science reaches maturity, however, scientists have encountered cases where the solvent molecules should be explicitly considered. The lower critical solution temperature (LCST) of polymer solutions is a typical example. In the LCST system, a polymer solution undergoes phase separation with increasing the temperature in contrast to the UCST-type. In many cases, the LCST phase separation occurs in pair with the UCST one for the polymer solution such as polystyrene/cyclohexane [11], polystyrene/ethyl formate [12], and poly(ethylene oxide) (PEO)/*t*-butyl acetate and PEO/water [13]. In polystyrene/cyclohexane, for example, the LCST phase boundary appears at a temperature region higher than the UCST boundary. After these findings, it has been considered that the LCST phase separation is common for polymer solutions. The Flory-Huggins model, however, cannot predict the existence of LCST, because the  $\chi$  parameter should decrease monotonically as the temperature goes up. Moreover, the enthalpy change in the LCST phase separation is generally positive (endothermic) because of desolvation. If only the mixing entropy ( $\Delta S_{\text{mix}}$ ) is taken into account, the endothermic phase separation seems strange, because the phase separation may lower the entropy of the system. In this case, we must consider the solvent as an ensemble of explicit molecules, in which the shape and volume of the solvents are important. This topic will be discussed in the later section with the hydrophobic interaction.

In a multicomponent system such as a biological solution, the solvation is sometimes inhomogeneous (see Fig. 11.1). The hydration of a solute becomes selective in a mixture of water and a less polar fluid, depending on whether the solute is hydrophilic or hydrophobic. The inhomogeneity of solvation arises from a large solvation Gibbs energy of each interactive site, which typically exceeds the thermal energy. The selective solvation affects the solution properties. For synthetic polymers, the selective solvation has been reported for poly(*N*-isopropylacrylamide) (PNiPAm) in ethanol with a tiny amount of water

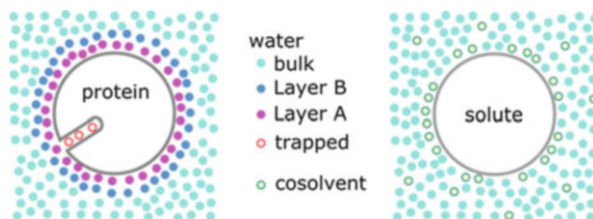


**Fig. 11.1** Schematic image of the inhomogeneous hydration. (Left) Hydration shell of proteins. (Right) Selective solvation in the case that the interaction between cosolvent and solute is larger than that between water and solute

[14] and poly(*N*-*n*-propylacrylamide) in water/isopropanol mixture [15]. These polyacrylamide derivatives undergo LCST phase separation in water, and the cosolvent modifies their solution properties.

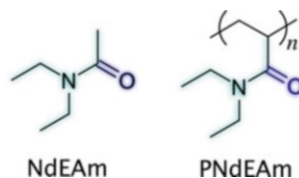
We need to consider explicit solvents not only for the selective solvation of synthetic polymers, but also for the hydration of proteins. The quantity of hydration water is 0.2–0.4 g per 1 g of proteins, which is broadly categorized into three types: internal water molecules that are trapped in internal cavities and deep clefts, water molecules that interact with the protein surface, and those loosely interacting with both the surface and the bulk water [16]. The schematic image is illustrated in Fig. 11.1. The hydration shell that consists of water molecules influenced by the protein surface plays a fundamental role in the activity of the protein [17]. In the hydration shell, there are at least two distinct hydration layers: strongly bounded water (layer A) and weakly bounded water (layer B). While the freezing point of bulk water is 0 °C, the water in layer B freezes at around –25 °C, and the water in layer A does not freeze until around –70 °C. The water molecules in the layer A are directly oriented to the charged and/or polar side chain of proteins, and thus its thermal motion is strongly constrained [18]. The rotational relaxation time ( $\tau_r$ ) of these water molecules is typically of the order of  $10^{-6}$  s. Because  $\tau_r \sim 10^{-12}$  for the bulk water, we can imagine how much the rotational motion is hindered in the layer A. On the other hand,  $\tau_r \sim 10^{-9}$  s is found for the water molecules in the layer B, which are hydrogen bonded with water molecules in the layer A. The water molecules in the layers A and B are not confined in each layer but are frequently replaced by thermal motions. When a third component, such as salt or sugar, is added to an aqueous protein solution, the hydration structure of the protein is perturbed, resulting in the destabilization of the protein. The hydration layers also play an important role in the synthetic polymers. It has been pointed out that the biocompatibility of polymeric materials is correlated with the existence of a specific hydration layer [19], referred to as the freezing-bound water that may correspond to the water molecules in the hydration shell of proteins.

The solvation of polymeric materials is complicated, as mentioned above, which makes their solution properties characteristic. Peculiar functions of polymeric compounds often originate from this characteristic solvation. In many cases, therefore, the explicit solvent is required to understand the solvation of polymers. In the following sections, we give some examples for the complicated solvation of polymers and also for the block design concept of the amphiphilic polymers.

## 11.2 Solvation of Polymers at Molecular Level

The vibrational spectroscopies, such as infrared (IR) and Raman, are powerful tools to investigate the solvation state of solutes at the molecular level. Even for the solvation of low-molecular-weight compounds, an explicit solvent model is required to understand the vibrational spectra. The very details of the solvation of low-molecular-weight compounds are found in the literature [20]. For acetamide

**Fig. 11.2** Chemical structures of *N,N*-diethylacetamide (NdEAm) and poly(*N,N*-diethylacrylamide) (PNdEAm)



compounds, the peak position of the C=O stretching vibration ( $\nu_{\text{C=O}}$ ) mode in the solution can be reproduced by assuming a direct interaction with solvent molecules [21]. In addition, we must take into account the effects of neighboring chains to interpret the solvation effects on vibration bands for polymeric compounds. The  $\nu_{\text{C=O}}$  bands of poly(*N,N*-diethylacrylamide) (PNdEAm) and its monomer model, *N,N*-diethylacetamide (NdEAm), give good examples to understand how the solvation at the molecular level is different between polymers and low-molecular-weight compounds. The chemical structures of NdEAm and PNdEAm are shown in Fig. 11.2. The IR spectra of NdEAm and PNdEAm are measured in water, methanol, ethanol, 1-propanol, acetone, THF,  $\text{CHCl}_3$ , and benzene, as shown in Figs. 11.3 and 11.4, respectively.

These  $\nu_{\text{C=O}}$  bands suggest that the dielectric constant ( $\epsilon$ ) of solvent plays a minor role, i.e., a continuum medium model cannot explain the change in these bands [20]. The  $\nu_{\text{C=O}}$  bands of NdEAm in acetone and 1-propanol are completely different even though  $\epsilon$  of these solvents is similar ( $\epsilon = 20.7$  for acetone and  $\epsilon = 20.1$  for 1-propanol); a unimodal peak is observed at  $1641\text{ cm}^{-1}$  in acetone, while three peaks appear at  $1655$ ,  $1628$ , and  $1605\text{ cm}^{-1}$  in 1-propanol. In  $\text{CHCl}_3$  ( $\epsilon = 4.81$ ), the  $\nu_{\text{C=O}}$  band appears at a lower frequency compared with those in THF ( $\epsilon = 7.6$ ) and benzene ( $\epsilon = 2.27$ ). Although  $\epsilon$  of alcohols varies from 13.3 to 32.66, the frequencies of three  $\nu_{\text{C=O}}$  peaks observed are almost identical. The bands at  $1626$ – $1630$  and  $1605\text{ cm}^{-1}$  are assignable to the C=O groups forming one and two hydrogen bonds, respectively. The band at  $1655\text{ cm}^{-1}$  likely originates from the C=O groups surrounded by alkyl groups of alcohols [20].

By comparing the  $\nu_{\text{C=O}}$  bands of PNdEAm and NdEAm in each solvent, some of them are similar, and some are different. The  $\nu_{\text{C=O}}$  band at the same position in the same solvent is supposed to have the same origin:  $1591\text{ cm}^{-1}$  (NdEAm)/ $1595\text{ cm}^{-1}$  (PNdEAm) in water,  $1626\text{ cm}^{-1}$  (NdEAm)/ $1628\text{ cm}^{-1}$  (PNdEAm) in  $\text{CHCl}_3$ , and  $1641\text{ cm}^{-1}$  (NdEAm)/ $1637\text{ cm}^{-1}$  (PNdEAm) in acetone. The other bands may reflect the difference in solvation between low-molecular-weight and polymeric compounds. A correlation plot of the  $\nu_{\text{C=O}}$  wavenumber for NdEAm versus that/those for PNdEAm in each solution is helpful to visualize the difference (Fig. 11.5). If the solvation state of C=O groups in NdEAm and PNdEAm is similar, the point will appear near the correlation line. Several peaks deviate from the line. The  $1616\text{ cm}^{-1}$  band in water is characteristically observed for PNdEAm, indicating that a part of C=O groups in PNdEAm is not sufficiently hydrated. Note that the fully hydrated C=O groups give rise to the band at  $1591$ – $1595\text{ cm}^{-1}$  for both NdEAm and PNdEAm. The neighboring side chains in PNdEAm may

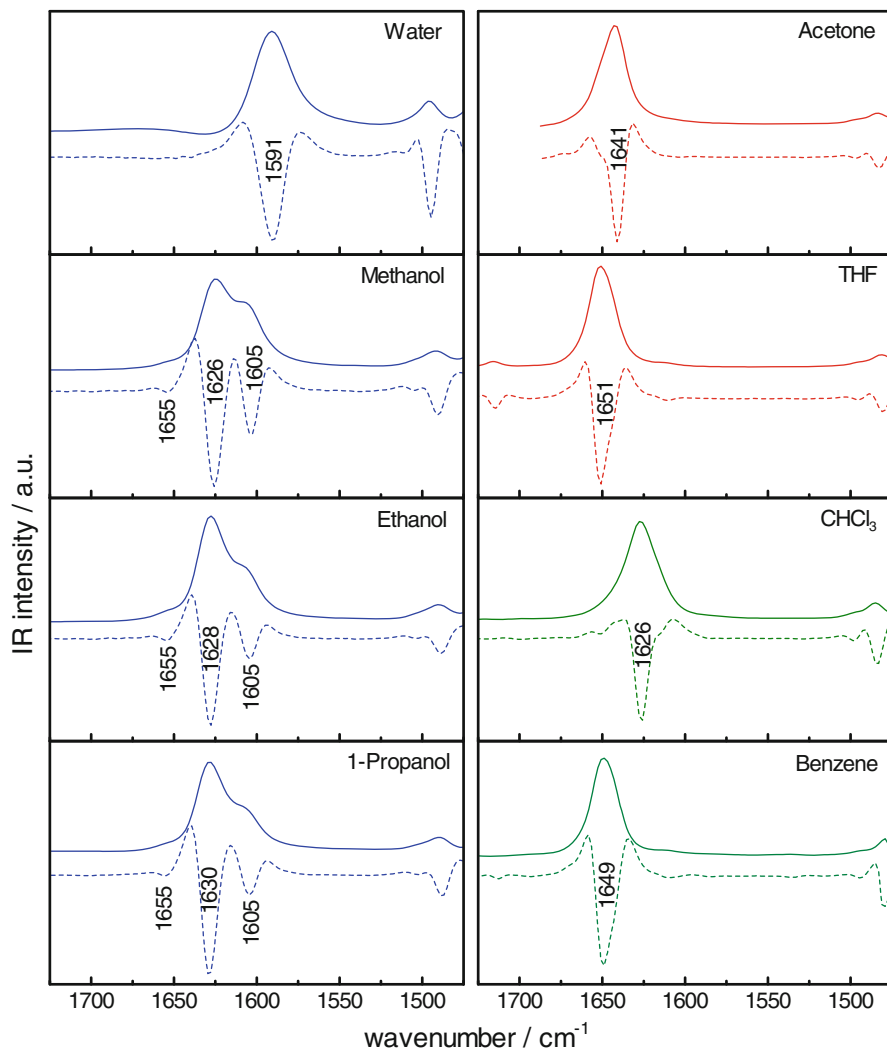


**Fig. 11.3** IR spectra of NdEAm in various solutions (solid lines) at the concentration of 0.2 M and their second derivatives (dotted lines). The colors indicate the polar protic solvents (blue), polar aprotic (red), and nonpolar aprotic (green) solvents. The original data of the figures are found in the reference [21]

interfere with the hydration. Interestingly, this  $\nu_{\text{C}=\text{O}}$  wavenumber is equal to that the lower peak in the alcohol at  $1618\text{ cm}^{-1}$ , which is assignable to the C=O groups accept two protons from solvent alcohols [21]. The bands at  $1591\text{--}1595\text{ cm}^{-1}$  in water is possibly owing to the cooperative hydration, where the hydrogen bond is strengthened by the repetition of hydrogen bonding [22]. The lower peak at  $1618\text{ cm}^{-1}$  for PNdEAm in alcohols is also associated with the steric hindrance

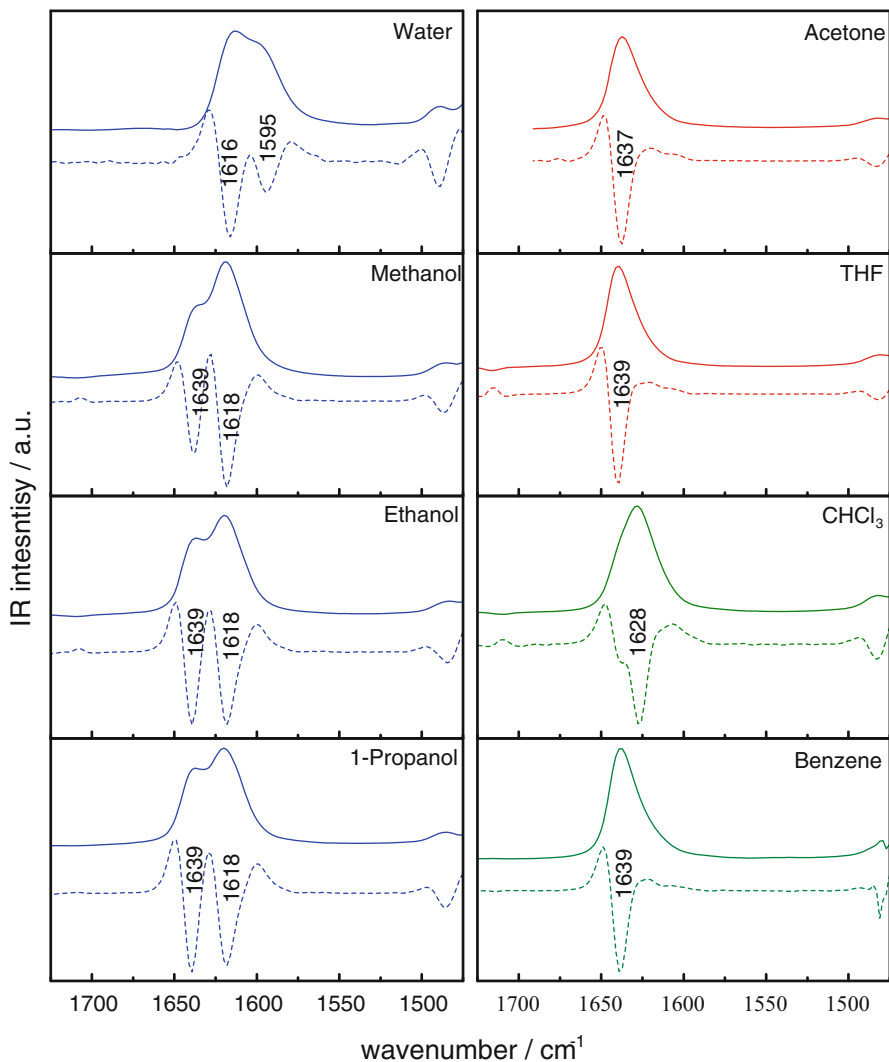


**Fig. 11.4** IR spectra of PNdEAm in various solutions (solid lines) at the concentration of 0.2 M and their second derivatives (dotted lines). The colors indicate the polar protic solvents (blue), polar aprotic (red), and nonpolar aprotic (green) solvents. The original data of the figures are found in the reference [21]

to solvation by the neighboring chain, because the wavenumber is markedly higher than the lowest peak at  $1605\text{ cm}^{-1}$  for NdEAm. On the other hand, the band at  $1639\text{ cm}^{-1}$  of PNdEAm in alcohols, THF, and benzene locates lower than the corresponding band of NdEAm. This indicates that the dipole interaction with the neighboring C=O groups causes the lower frequency shift in the C=O groups in polymers [23].

**Fig. 11.5** Correlation plot of the peak position(s) of the C=O stretching band for NdEAm versus that/those for PNdEAm in each solvent. The colors indicate the polar protic solvents (blue), polar aprotic (red), and nonpolar aprotic (green) solvents. The original data of the figures are found in the reference [21]

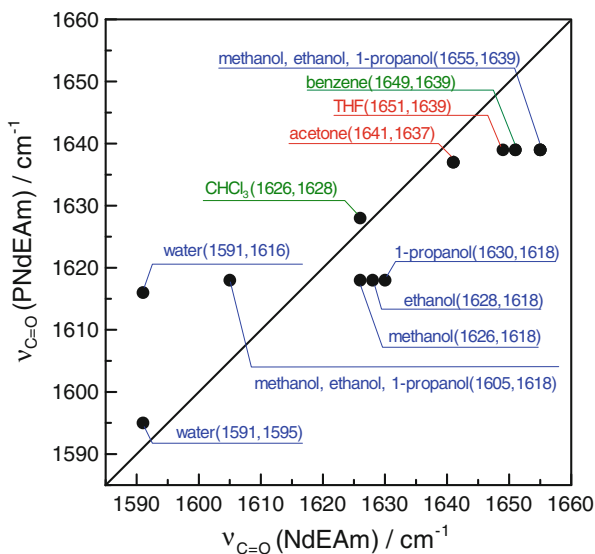
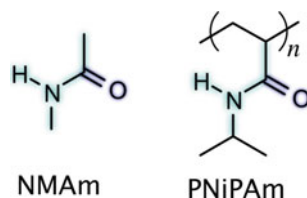


**Fig. 11.6** Chemical structures of *N*-methylacetamide (NMAM) and poly(*N*-isopropylacrylamide) (PNiEAm)



The effects of the intramolecular interaction on the solvation of polymers possibly become more significant if the polymers have both the hydrogen donor and acceptor. The intramolecular hydrogen bond of biopolymers, which is often competitive with hydration, is responsible for the higher order structures, as can be seen for proteins and nucleic acids. The solvation of poly(*N*-isopropylacrylamide) (PNiPAm) gives a model case, because the side chain has not only the hydrogen acceptor (C=O group) but the hydrogen donor (N-H group). Figure 11.6 shows the chemical structures of PNiPAm and its monomer model compound, *N*-methylacetamide (NMAM). The vibration modes of secondary amide groups are complicated. In vacuum, there are two characteristic vibration modes in the 1700–1500  $\text{cm}^{-1}$  region, namely, the amide I and II modes (referred to as  $\nu_{\text{am I}}$  and  $\nu_{\text{am II}}$ , respectively). The  $\nu_{\text{am I}}$  mode is mainly due to  $\nu_{\text{C=O}}$  (80%), while the  $\nu_{\text{am II}}$  mode is due to the coupling between the N-H bending (60%) and C-N stretching (40%) vibrations [24].

Figure 11.7 shows IR spectra in the 1725–1475  $\text{cm}^{-1}$  region of PNiPAm in various solvents together with the curve-fitting results. PNiPAm in water undergoes the LCST phase separation, where the cloud point ( $T_c$ ) is near 32 °C. Thus, the IR spectrum was also measured above and below  $T_c$ . Prominent bands in Fig.



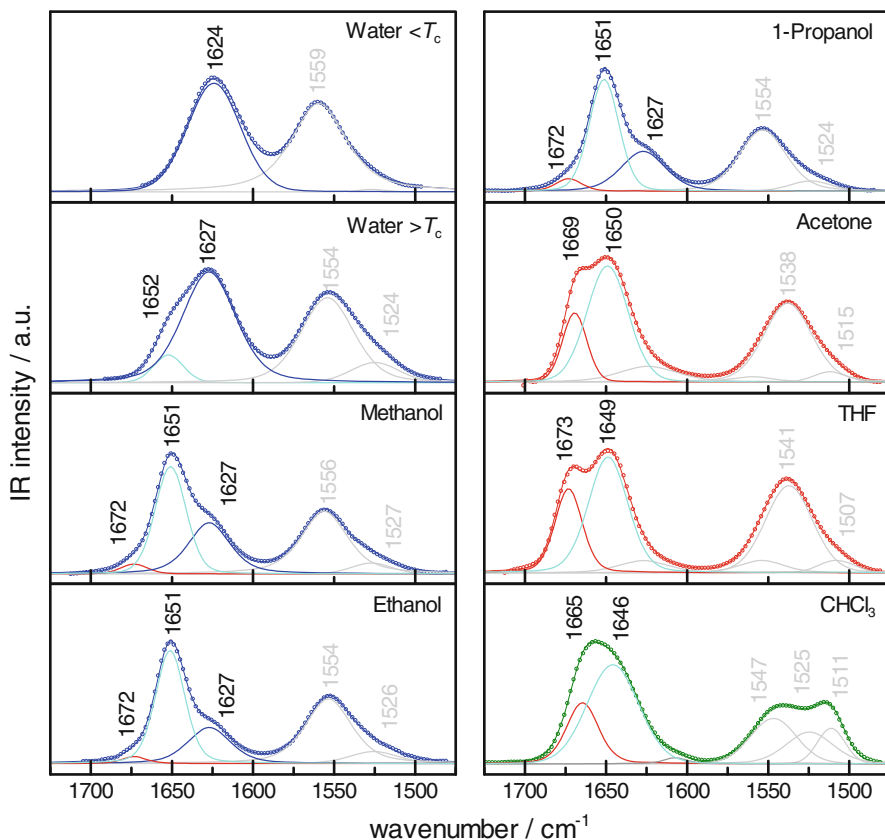


**Fig. 11.7** IR spectra of PNIPAM in the 1725–1475  $\text{cm}^{-1}$  region observed for the various solutions (open circles) and curve-fitting results (solid lines). The Voigt function is used in the fitting procedure with the non-linear least square method. The colors of open circles indicate the polar protic solvents (blue), polar aprotic (red), and nonpolar aprotic (green) solvents. The colors of solid lines represent the band region; (red) 1672–1660  $\text{cm}^{-1}$ , (light blue) 1652–1646  $\text{cm}^{-1}$ , and (blue) 1627–1624  $\text{cm}^{-1}$

11.7 are due to the  $\nu_{\text{am I}}$  and  $\nu_{\text{am II}}$  modes. The peak positions and band shapes of the amide bands strongly depend on the solvents. Hereafter, we focus on the  $\nu_{\text{am I}}$  bands, which show a similar change with the  $\nu_{\text{C=O}}$  band of PNDEAm (Fig. 11.4). The variation in the  $\nu_{\text{am I}}$  bands of PNIPAM is similar to that in the  $\nu_{\text{C=O}}$  bands of PNDEAm. The lowest  $\nu_{\text{am I}}$  peak locates at 1624–1627  $\text{cm}^{-1}$  in water and alcohols, which corresponds to the 1616–1618  $\text{cm}^{-1}$  peaks of PNDEAm. For the alcohols, the band at 1651  $\text{cm}^{-1}$  becomes prominent, indicating that the  $\text{C=O}\cdots\text{H-O}$  interaction in alcohols is weaker than that of water. This band should have the same origin of the shoulder peak at 1652  $\text{cm}^{-1}$  observed in water above  $T_c$ . The origin of the 1652  $\text{cm}^{-1}$  band is concerned not only with the dehydration but also with the changes in the intramolecular  $\text{C=O}\cdots\text{H-N}$  interaction [25]. In acetone and

THF, there are at least two peaks in the  $\nu_{\text{am I}}$  band envelope for PNiPAm, while only one peak appears for PNdEAm. This should be associated with the existence of  $\text{C}=\text{O}\cdots\text{H}-\text{N}$  interaction among the neighboring chains of PNiPAm. While the intramolecular interaction among the side chain of PNdEAm makes only the  $\nu_{\text{C}=\text{O}}$  band shift to a lower frequency as mentioned above, that of PNiPAm causes a new band at a lower wavenumber region. This simply shows how the hydrogen bond among the side chain gives rise to a significant effect on the corresponding IR bands. The highest  $\nu_{\text{am I}}$  peak is observed at around  $1669\text{--}1673\text{ cm}^{-1}$  in acetone and THF.

The  $\nu_{\text{am I}}$  and  $\nu_{\text{am II}}$  regions of NMAM in various solvents are represented in Fig. 11.8. The spectral variation resembles that of PNiPAm. Note that the  $\nu_{\text{am I}}$  wavenumber of NMAM is intrinsically higher by ca.  $10\text{ cm}^{-1}$  than that of *N*-

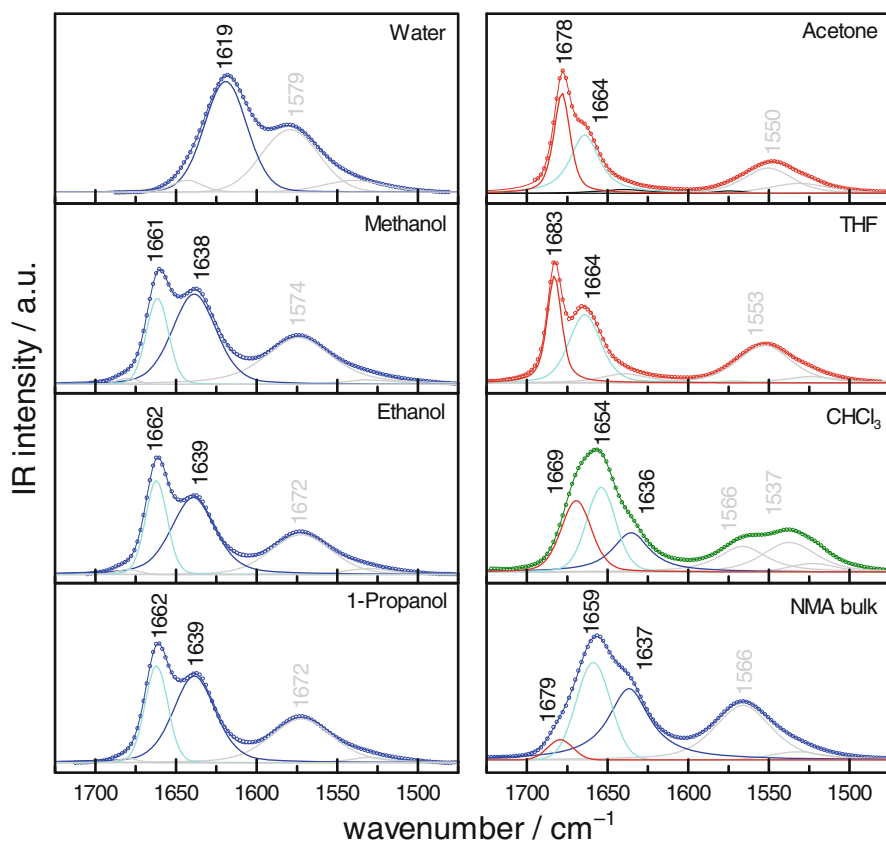
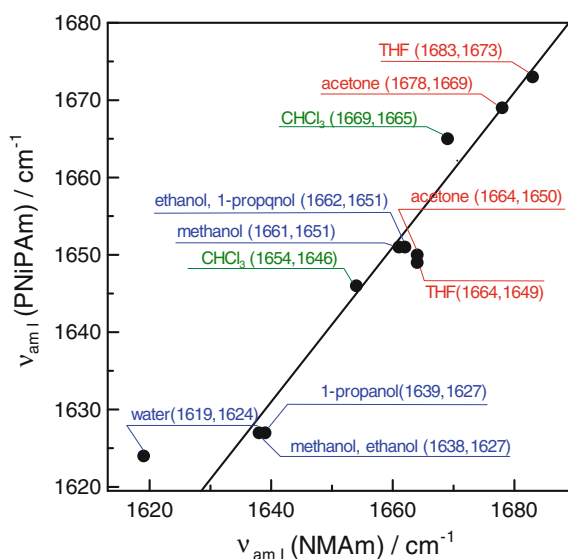


**Fig. 11.8** IR spectra of NMAM in various solutions at the concentration of 0.27 M (open circles) and curve-fitting results (solid lines). The Voigt function is used in the fitting procedure with the non-linear least square method. The colors of open circles indicate the polar protic solvents (blue), polar aprotic (red), and nonpolar aprotic (green) solvents. The colors of solid lines represent the band region; (red)  $1672\text{--}1660\text{ cm}^{-1}$ , (light blue)  $1652\text{--}1646\text{ cm}^{-1}$ , and (blue)  $1627\text{--}1624\text{ cm}^{-1}$

isopropylacetamide [26] because of the difference between methyl and isopropyl groups attached to *N* atom. If their solvation state is similar, the  $\nu_{\text{am I}}$  wavenumber of PNiPAm should be lower by ca.  $10 \text{ cm}^{-1}$  than that of NMAm. By comparing Figs. 11.3 and 11.8, we can consider that the solvation effect on the  $\nu_{\text{am I}}$  band of NMAm is similar with that on the  $\nu_{\text{C=O}}$  band for NdEAm. However, there are also some differences. For example, in acetone and THF there are at least two peaks in the  $\nu_{\text{am I}}$  band envelope for NMAm, whereas only one  $\nu_{\text{C=O}}$  peak is found for NdEAm. This possibly originates from the multimer complex of NMAm formed by an intermolecular  $\text{C=O}\cdots\text{H-N}$  hydrogen bond. The number and wavenumber of the  $\nu_{\text{am I}}$  peaks of NMAm are almost identical for alcohol solutions and the neat liquid. That is, the bands due to the  $\text{C=O}\cdots\text{H-N}$  or  $\text{C=O}\cdots\text{H-O}$  hydrogen bond gives a clear, isolate band, resulting in the multicomponent  $\nu_{\text{am I}}$  envelope. The similarity of the  $\nu_{\text{am I}}$  wavenumber for each peak in alcohols and bulk suggests that the hydrogen bond strength is equivalent. Therefore, it is quite difficult to distinguish whether a  $\nu_{\text{am I}}$  peak arises from the  $\text{C=O}\cdots\text{H-N}$  hydrogen bond or from the  $\text{C=O}\cdots\text{H-O}$  hydrogen bond.

In Fig. 11.9, the wavenumber of the  $\nu_{\text{am I}}$  peak for NMAm in each solvent is plotted against that for PNiPAm. The correlation is fairly good, which may include the contribution of inter- or intramolecular  $\text{C=O}\cdots\text{H-N}$  hydrogen bonds in addition to the solvation effects. Interestingly, the correlation for NMAm/PNiPAm seems to be much better than that of NdEAm/PNdEAm. We have supposed that the formation of the intermolecular  $\text{C=O}\cdots\text{H-N}$  hydrogen bond among NMAm in solution results in a similar spectral variation with PNiPAm, in which the side chains form the intramolecular  $\text{C=O}\cdots\text{H-N}$  hydrogen bond. The exception is found for water. The  $\nu_{\text{am I}}$  peak of PNiPAm in water at  $1624 \text{ cm}^{-1}$  is much higher than the

**Fig. 11.9** A correlation plot of the peak position(s) of the  $\nu_{\text{am I}}$  band for NMAm versus that(those) for PNiPAm in each solvent. The solid line was drawn by  $\nu_{\text{am I}}$  (PNiPAm) =  $\nu_{\text{am I}}$  (NMAm) - 9 as guides to the eye. The colors of notes correspond to the polar protic solvents (blue), polar aprotic (red), and nonpolar aprotic (green) solvents



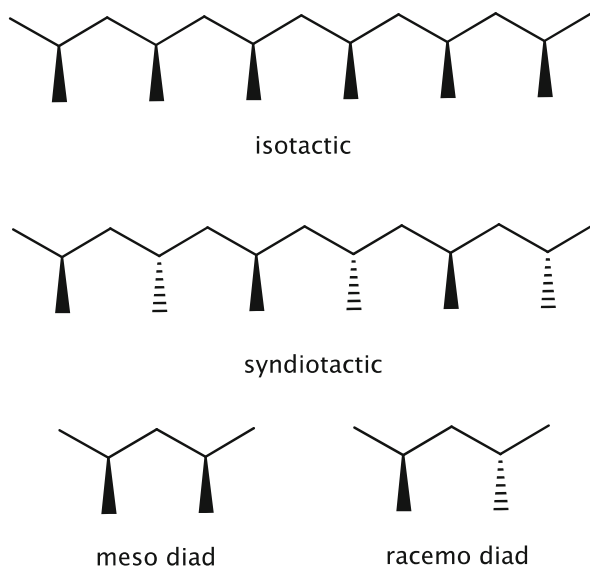
expectation ( $\sim 1610\text{ cm}^{-1}$ ). Indeed, the  $\nu_{\text{am I}}$  band at  $1601\text{ cm}^{-1}$  is observed for *N*-isopropylpropionamide in water [27]. Thus, we consider that the C=O groups of PNiPAm in water are not fully hydrated. Although the insufficient hydration of the C=O groups is also observed for PNdEAm, the shield of C=O groups from water seems to be more significant for PNiPAm. The correlation line suggests that the existence of fully hydrated C=O groups of PNiPAm should give the  $\nu_{\text{am I}}$  band at  $1610\text{ cm}^{-1}$ . However, no peak appears at a lower wavenumber than  $1620\text{ cm}^{-1}$  in actuality. The difference between PNdEAm and PNiPAm is the possibility to form a C=O $\cdots$ H-N hydrogen bond between neighboring amide groups. Therefore, we have assumed that the hydration for the side chain of PNiPAm is suffered from the intramolecular C=O $\cdots$ H-N hydrogen bond. Hydrogen-deuterium (H-D) exchange experiments for PNiPAm and its model compounds reveal that the amide groups incorporated in the side chain of PNiPAm form an intramolecular C=O $\cdots$ H-N hydrogen bond even in a good solvent [28].

We now understand the fact that the solvation of polymeric compounds is complicated, which requires explicit solvent molecules to understand. The solvation of the polymer chain is remarkably influenced by the neighboring chain in many cases.

### 11.3 How the Intramolecular Interactions Affect the Properties of Polymers in Solution

The effects of stereoregularity of polymers on the solution properties are interesting because the relationship among the side chain should be perturbed by the configuration. Tacticity is the relative stereochemistry of adjacent chiral centers within a vinyl polymer (Fig. 11.10). The PNiPAm and PNdEAm are vinyl polymers whose aqueous solutions undergo the LCST phase separation. The chemical structure of vinyl polymers is represented as  $(\text{CH}_2\text{-CH}(\text{R}))_n$ , where the carbon connecting with the side chain R becomes the chiral center. In an isotactic polymer, all the side chains are located on the same side of the backbone, while in a syndiotactic polymer, the side chains locate alternatively along the chain. For a synthetic polymer, in general, the side chains have a random position referred to as atactic. These relative positions of side chains cannot be exchanged by the rotation of the backbone. That is, the tacticity of a polymer is intrinsic. In the simplest case, the relative position of two adjacent units (diad) is used to characterize the stereoregularity of polymers. If the orientation of the two units is the same, the diad is “meso,” while the alternative orientation is referred as “racemo.”

PNiPAm and PNdEAm obtained from a radical polymerization are generally atactic. If the tacticity of the polymers is modified, the intramolecular interaction among the neighboring chains should be influenced. In the last two decades, many efforts have been made for controlling the tacticity in radical polymerization [29]. Several researchers have recently suggested that the tacticity modifies the

**Fig. 11.10** Tacticity of vinyl polymers**Table 11.2** Diad tacticity,  $M_n$ , and  $M_w/M_n$  of stereocontrolled PNiPAm

ID	$m:r$	$M_n/10^4 \text{ g mol}^{-1}$	$M_w/M_n$
PNiPAm- <i>m</i> 46	46: 54	3.2	1.21
PNiPAm- <i>m</i> 60	60: 40	3.0	1.30
PNiPAm- <i>m</i> 64	64: 36	3.4	1.29

**Table 11.3** Diad tacticity,  $M_n$ , and  $M_w/M_n$  of stereocontrolled PNdEAm

ID	$m:r$	$M_n/10^4 \text{ g mol}^{-1}$	$M_w/M_n$
PNdEAm- <i>m</i> 58S	58:42	5.1	1.25
PNdEAm- <i>m</i> 68S	68:32	5.2	1.28
PNdEAm- <i>m</i> 82S	82:18	4.7	1.23
PNdEAm- <i>m</i> 55L	55:45	17.0	1.66
PNdEAm- <i>m</i> 75L	75:25	15.0	1.68

cloud point ( $T_c$ ), or the phase separation temperature, of the aqueous solution of polyacrylamides. Ray et al. have found that  $T_c$  of the PNiPAm aqueous solution decreases with increasing the meso diad ( $m$ ) content of the polymer [30]. On the contrary, Hirano et al. revealed that  $T_c$  goes up with the increase in the racemo diad ( $r$ ) content of PNiPAm [31]. For the aqueous solution of PNdEAm, the tacticity effects on  $T_c$  have been reported by Freitag et al. [32] and Kobayashi et al. [33]. The number average molecular weight ( $M_n$ ), the polydispersity index ( $M_w/M_n$ , where  $M_w$  is the weight average molecular weight), and the diad tacticity ( $m:r$ ) of PNiPAm and PNdEAm, which are prepared by a reversible addition-fragmentation chain-transfer (RAFT) polymerization with metal trifluoromethanesulfonates, were listed in Tables 11.2 and 11.3. The details of preparation can be found in elsewhere [34, 35].

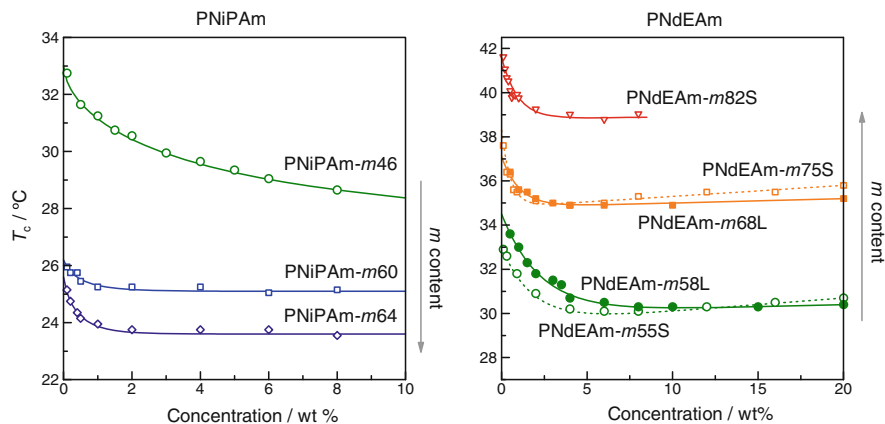
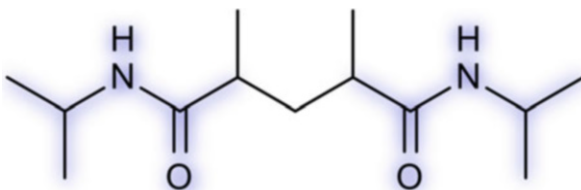


**Fig. 11.11** (Left)  $T_c$  plotted against the concentration of PNiPAm-*m*46 (open circles), PNiPAm-*m*60 (open rectangles), and PNiPAm-*m*64 (open diamonds) in water. (Right)  $T_c$  plotted against the concentration of PNdEAm-*m*55S (open circles), PNdEAm-*m*68S (open rectangles), PNdEAm-*m*82S (open triangle), PNdEAm-*m*55L (closed circles), and PNdEAm-*m*75L (closed rectangles) in water. The solid lines are drawn as guides to the eye. The original data of the figures are found in the reference [34, 35]

The left panel of Fig. 11.11 represents the phase boundary for the aqueous solutions of PNiPAm-*m*46, PNiPAm-*m*60, and PNiPAm-*m*64, which are estimated by plotting  $T_c$  against the polymer concentration [34]. For PNiPAm-*m*46,  $T_c$  monotonically decreases from ca. 33 to 29 °C as the polymer concentration increases. The critical point cannot be determined in this concentration region on account of the shape of the phase boundary curve. This tendency is similar to that reported previously for an atactic PNiPAm [36]. The lack of the minimum in the phase boundary for the PNiPAm/water system has been controversial [37, 38]. The tacticity significantly affects the phase boundary curve for the PNiPAm aqueous solution, which shifts to lower temperature with increasing *m*. That is, PNiPAm becomes hydrophobic when the *m* content increases.

The phase boundary of PNiPAm-*m*60 and PNiPAm-*m*64 becomes flat at a higher concentration regions. Okada and Tanaka have theoretically predicted that the phase boundary curve shifts to lower temperature with changing its shape from a convex downward form to concentration-independent, flat shape when the cooperativity of hydration increases [39]. Because the water molecule has both donor and acceptor sites of hydrogen bonds, they may form zipper-like, cooperative hydrogen bonds around the polymer chains. Under this situation, the dehydration of one water molecule has the domino effect to trigger the dehydration of others (this is the same for hydration), resulting in lowering  $T_c$ . If the cooperativity of hydration becomes stronger, the phase boundary will decrease monotonically as the concentration of polymer increases. Therefore, we presumed that the tacticity affects not only the hydrophobicity of the chain but also the cooperativity of hydration.

**Fig. 11.12** Chemical structure of a dimer model compound of PNiPAm (dNiPAm)



The results indicate the hydrophilicity (or hydrophobicity) of PNiPAm is significantly modified by the tacticity. Indeed, the stereoisomers of the dimer model compound, *N,N'*-diisopropyl-2,4-dimethylglutaryl amide (dNiPAm, Fig. 11.12), have different solubility to water [40]; dNiPAm with racemo configuration (*r*-dNiPAm) is more soluble in water than dNiPAm with meso configuration (*m*-dNiPAm). Although the difference of the hydration Gibbs energy between *m*- and *r*-dNiPAm is not large ( $\sim 1.2 \text{ kJ mol}^{-1}$ ), the 5% difference in the *m* content would cause a large difference in the solubility for the whole chain of PNiPAm (300 monomer units for  $c = 3.4 \times 10^4 \text{ g mol}^{-1}$ ).

The water-solubility of PNdEAm also depends on its tacticity. The right panel of Fig. 11.11 represents the phase boundary for the stereocontrolled PNdEAm in water [35]. Regardless of the molecular weight, the phase boundary curve shifts to higher temperatures with increasing *m*. The tendency is opposite to the PNiPAm/water system. Interestingly, the shape of the phase boundary of PNdEAm in water is not sensitive to the tacticity, unlike that of PNiPAm in water. At a higher concentration, the phase boundary of PNdEAm in water becomes flat, which is similar to those of the PNiPAm-*m*60 and -*m*64 in water. This may also be concerned with the cooperative hydration of PNdEAm chains. Though the 1 ~ 2 wt% aqueous solution of both atactic PNiPAm and PNdEAm has  $T_c$  around 31 °C, their phase separation behaviors are different in some aspects. In the thermogram of the differential scanning calorimetry, the peak arising from the phase separation of PNdEAm/water is remarkably broad compared with that for PNiPAm/water [41]. PNiPAm in water shows the hysteresis in demixing and remixing processes, while PNdEAm does not. In the coil-globule transition of PNiPAm single chain in water, the gyration and hydrodynamic radii of PNiPAm chains in the globule-to-coil transition (cooling process) are always smaller than those in the coil-to-globule transition (heating process) [42]. These differences possibly originate from the fact that PNiPAm forms an intramolecular hydrogen bond among the amide groups [43]. On the other hand, no hysteresis occurs in the coil-globule transition of PNdEAm in water [44].

The tacticity affects the phase boundary of the aqueous solutions of both PNiPAm and PNdEAm in water. However, the effects of the *m* content are opposite; PNiPAm chains seem to be hydrophobic with increasing *m*, while PNdEAm chains are hydrophilic. As we discussed in the previous section, the intramolecular interaction among the side chains is different between PNiPAm and PNdEAm. In the current state, however, we have only the circumstantial evidence for the solvation state of these polymers. The quantum chemical calculations of the solvation energy

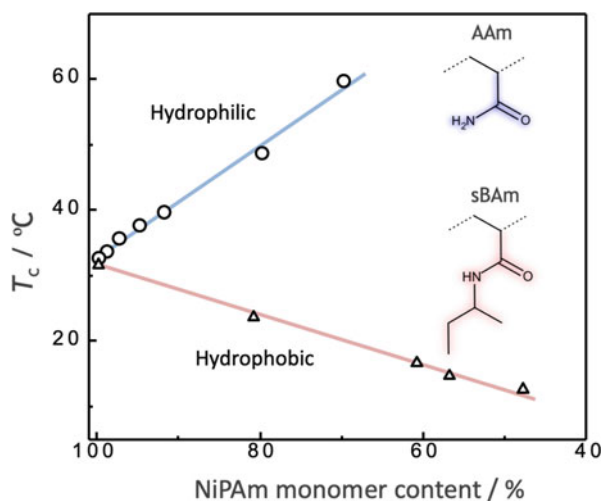
for large, polymeric compounds with an explicit solvent model are still under development.

## 11.4 Block Design of Amphiphilic Copolymers

The hydrophobic interaction plays an important role not only in the self-assembly of synthetic amphiphilic polymers but also in protein folding. The amphiphilicity, the hydrophilic-hydrophobic balance, is crucial. The hydrophobic parts induce the assembling of the molecules in aqueous media, while the hydrophilic moieties work as solubilizer to the media.

Synthetic amphiphilic polymers are widely used in industrial applications as emulsifiers and viscosity modifiers. The self-assembly of non-ionic amphiphilic polymers is often triggered by heat. These thermoresponsive polymers are indispensable as building blocks of smart, intelligent materials. The way to control the amphiphilicity of polymers is the copolymerization of hydrophilic and hydrophobic monomers with an appropriate balance. In some cases, the random copolymerization has worked well. Figure 11.13 shows the changes in  $T_c$  of the aqueous solution of PNiPAM-based random copolymers depending upon the comonomer ratio. Acrylamide (AAm) monomer is more hydrophilic than NiPAM, whereas *N*-*sec*-butylacrylamide (sBAAm) is more hydrophobic.  $T_c$  of PNiPAM-based copolymer descends when sBAAm is copolymerized [45], while that elevates with AAm [46]. The change in  $T_c$  is proportional to the comonomer content, indicating that the hydrophilic-hydrophobic balance is predictable by the comonomer ratio. On the other hand, there are also undesirable cases, where the property of AB random copolymer unexpectedly deviates from those of A and B homopolymers. The

**Fig. 11.13**  $T_c$  of the aqueous solution of PNiPAM-based copolymers plotted against the comonomer ratio; poly(acrylamide) (open circles) and poly(*N*-*sec*-butylacrylamide) (open triangles). The solid lines are drawn as guides to the eye. The original data of the figures are found in the reference [45, 46]





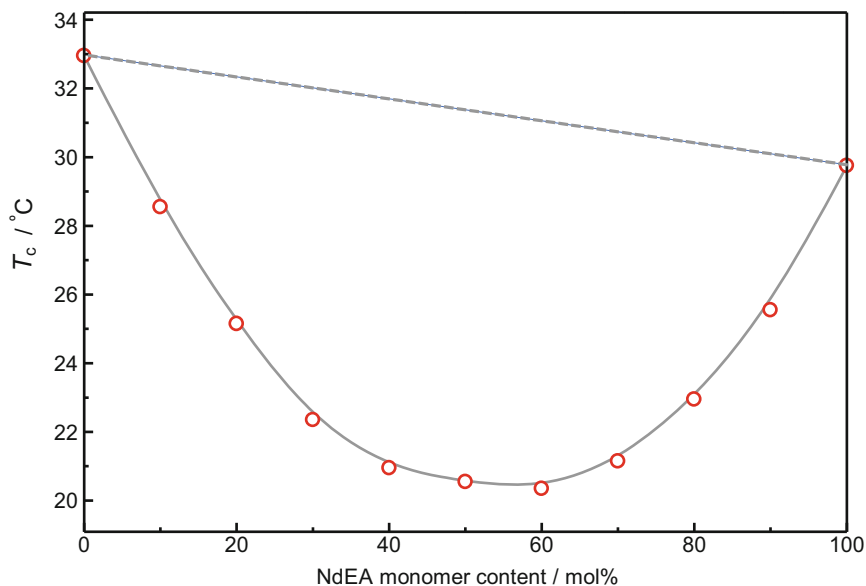


**Fig. 11.14**  $T_c$  of the aqueous solution of poly(NiPAm-co-NdEAm) plotted against the NdEAm monomer ratio in PNiPAm-based copolymers. The solid and dotted lines are drawn as guides to the eye

copolymerization of NiPAm and NdEAm gives a crucial example [47–49]. Figure 11.14 shows  $T_c$  of the aqueous solution of NiPAm/NdEAm random copolymers, poly(NiPAm-co-NdEAm), as a function of the NdEAm ratio. Although both PNiPAm and PNdEAm homopolymers possess  $T_c$  around 30–33 °C,  $T_c$  of a random copolymer of NiPAm and NdEAm with any composition is much lower. This phenomenon cannot be explained without considering the intramolecular interaction between neighboring NiPAm and NdEAm monomers in the chain. It is likely that the NiPAm-NiPAm and NdEAm-NdEAm sequences are more hydrophilic than the NiPAm-NdEAm sequence. Because the 3D structure of proteins is based on the primary structure, which is the sequence of the monomer units along the polymer chain, many efforts have been devoted to control the monomer sequence of synthetic polymers [50]. However, the solvation state of comonomers is unexpectedly modified by the neighboring chain as mentioned above. It means that the control of the monomer sequence may not always promise a desirable feature of the resulting polymers.

The design of the block sequence in multiblock copolymers could be an alternative strategy. In this method, an amphiphilic polymer can be built up by hydrophobic and hydrophilic homopolymer blocks. The block design becomes more effective when well-characterized homopolymers are employed as the building blocks. Under this strategy, we do not need to worry about unexpected, undesirable effects arising

from the neighboring interaction between comonomers. Several researchers have reported the preparation of multiblock copolymers such as pentablock copolymers based on poly(ethylene oxide) (PEO)-poly(propylene oxide) (PPO)-PEO triblock copolymer (Pluronic) [51–54]. The most important feature is the fact that these pentablock copolymers retain the solution property of each building block. For instance, a pH-responsive pentablock copolymer has been obtained by copolymerizing poly(2-(*N,N*-diethylamino)ethyl methacrylate) at both ends of Pluronic [52].

The basic idea to utilize hydrophobic interaction to assembling polymer chain is concerned with the depletion force. The depletion force causes the LCST phase separation of an aqueous solution. In general, a solute becomes more soluble to solvent at a higher temperature because of the mixing entropy ( $-T\Delta S_{\text{mix}} < 0$ ). Because the phase separation causes the decrease in the mixing entropy  $\Delta S_{\text{mix}}$ , the LCST phase separation should not be owing to  $\Delta S_{\text{mix}}$ . In the past, it has been supposed that the hydrophobic interaction is associated with the “ordered structure of water” around the hydrophobic moiety, which lowers the orientational entropy of the system. If the increment of the orientational entropy by the disorientation of water overcomes  $\Delta S_{\text{mix}}$ , the spontaneous phase separation may occur. However, the ordered structure of water around the hydrophobic moieties has been hardly detected in the liquid phase, even though many efforts have been devoted [55]. The depletion force is based on a more realistic mechanism. Around the hydrophobic moiety in aqueous media, there is an excluded volume where the water molecules cannot occupy. When the hydrophobic moieties are gathered, the excluded volume is reduced, results in the gain of the translational entropy of water. The depletion force among hydrophobic moieties also plays an important role in protein folding [56]. In the folding process from a random coil to a native structure, the conformational entropy of the chain decreases drastically. Although the formation of the stable higher structures yields a negative enthalpy, this is not enough to induce a spontaneous folding of the protein. The compensation arises from the association of hydrophobic domain in the chain, increasing in the translational entropy of water.

Here, we show two examples of the alternating block architecture for amphiphilic copolymers: PEO-PPO and PEO-PNiPAM alternating multiblock (AMB) copolymers (Fig. 11.15). In the PEO-PPO AMB copolymer, the hydrophilic PEO and hydrophobic PPO blocks connect alternatively, and the polymer becomes amphiphilic. Among the hydrophobic blocks in water, the depletion force works. PEO-PPO AMB copolymers undergo micellization in water like non-ionic surfactants and Pluronic. The aqueous solutions exhibit the LCST phase separation [57, 59]. Figure 11.16 represents the concentration dependences of micellization temperature ( $T_{\text{mic}}$ ) for the two types of PEO-PPO AMB copolymers in the water together with the phase separation curves. These copolymers are denoted as  $(\text{EO}_{220}\text{PO}_{33})_6$  and  $(\text{EO}_{68}\text{PO}_{33})_{10}$ , where EO is the ethylene oxide unit, PO is the propylene oxide unit, and the subscript is the number of repeating units. The weight fractions of PEO in a single chain ( $f_{\text{PEO}}$ ) of  $(\text{EO}_{220}\text{PO}_{33})_6$  and  $(\text{EO}_{68}\text{PO}_{33})_{10}$  are similar to Pluronic F88 ( $\text{EO}_{100}\text{PO}_{39}\text{EO}_{100}$ ) and P85 ( $\text{EO}_{25}\text{PO}_{39}\text{EO}_{25}$ ), respectively.

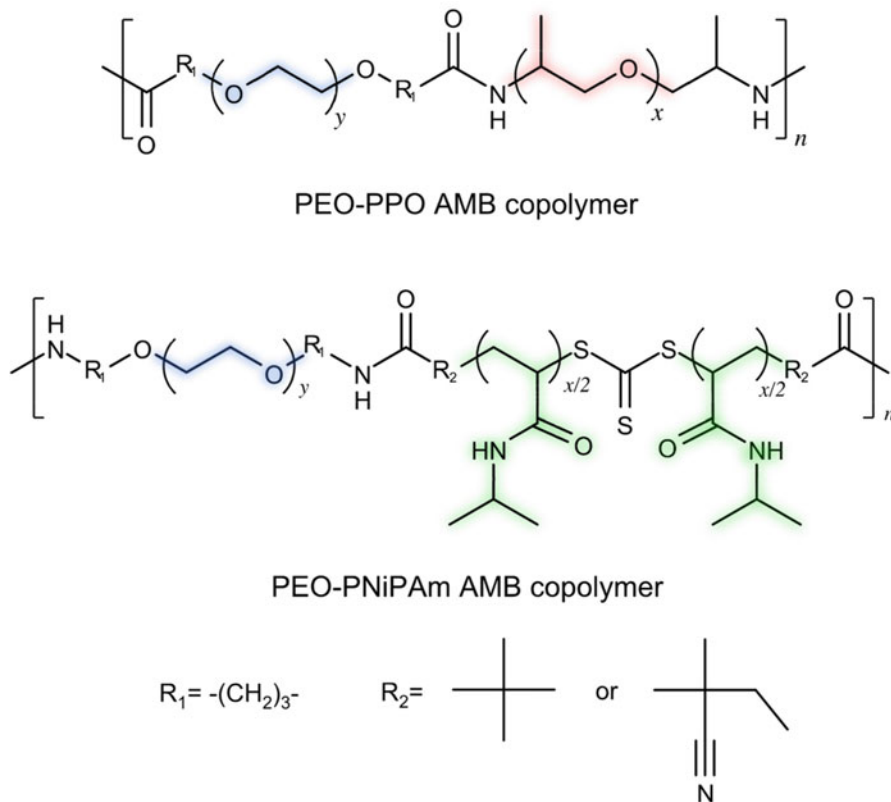


**Fig. 11.15** Chemical structures of PEO-PPO and PEO-PNiPAm AMB copolymers

Because Pluronic, a PEO-PPO-PEO triblock copolymer, is one of the most widely used and investigated polymeric surfactants [60, 61], it is interesting to compare their solution properties with those of the AMB copolymers.  $T_{\text{mic}}$  of the PEO-PPO AMB copolymer is slightly lower than that of Pluronic, having a similar  $f_{\text{PEO}}$ . Interestingly, the  $(\text{EO}_{220}\text{PO}_{33})_6$  and  $(\text{EO}_{68}\text{PO}_{33})_{10}$  aqueous solutions undergo phase separation at 40–80 °C, while Pluronic F88 ( $\text{EO}_{100}\text{PO}_{39}\text{EO}_{100}$ ) and P85 ( $\text{EO}_{25}\text{PO}_{39}\text{EO}_{25}$ ) in water have no  $T_c$  below 100 °C. Below  $T_{\text{mic}}$ , the unimer of the PEO-PPO AMB copolymer forms a core-corona structure, and then a multimer micelle appears with increasing temperature [57]. These behaviors suggest that the PPO blocks in the AMB copolymer are assembled in the aqueous medium to form unimer or multimer micelles through the hydrophobic interaction.

By using PNiPAm as a second block, we can build up a PEO-PNiPAm AMB copolymer [62]. As shown in the previous section, the hydrophobicity of PNiPAm can be modified by controlling  $m$  content. Thus, we prepare stereocontrolled

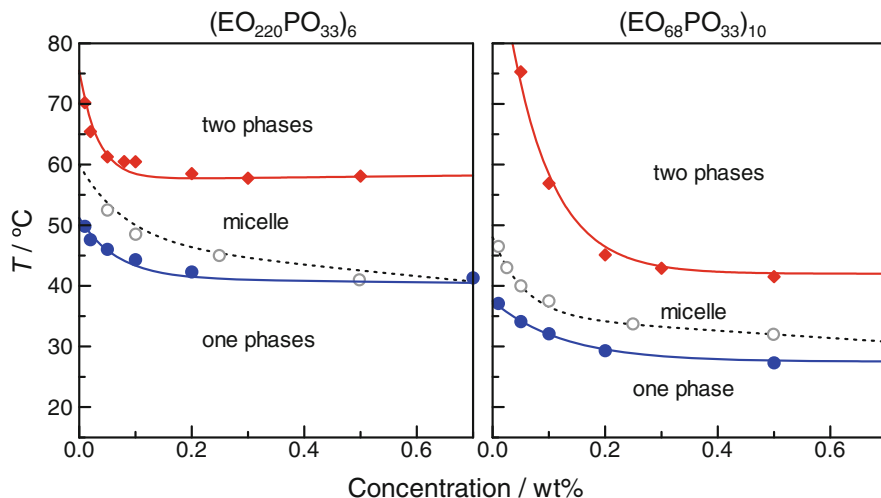


**Fig. 11.16** Phase diagram of the aqueous solution of (left)  $(EO_{220}PO_{33})_6$  and (right)  $(EO_{68}PO_{33})_{10}$ . The closed diamonds show  $T_c$ , and the closed circles represent  $T_{mic}$ . The original data of the figures are found in the reference [57]. The open circles indicate  $T_{mic}$  of Pluronic F88 and P85 found in the reference [58]. The solid and dotted lines are drawn as guides to the eye

PNiPAMs with  $m = 45, 50,$  and  $58\%$  (referred to as PNiPAM- $m45$ , PNiPAM- $m50$ , and PNiPAM- $m58$ , respectively). Although the aqueous solution of homopolymers of PNiPAM experiences the LCST phase separation, that of PEO-PNiPAM AMB copolymers does not. This implies that the PEO chains prevent the PNiPAM chains from assembling. The coil expansion of the AMB copolymers is influenced by changing the hydrophobicity of PNiPAM chains. Near room temperature, the PEO-PNiPAM AMB copolymers exist as a unimer. The unimer of PEO-PNiPAM- $m45$  in water behaves as an extended coil, whereas those of PEO-PNiPAM- $m50$  and PEO-PNiPAM- $m58$  shrink slightly, because the hydrophobicity of PNiPAMs depends on the  $m$  content. As the temperature goes up, all the AMB copolymers form multimer micelles. The apparent  $M_w$  determined by the static light scattering (SLS) reveals clearly the temperature dependence as shown in Fig. 11.17, where the second virial coefficient ( $A_2$ ) is also plotted. The increment of the apparent  $M_w$  near  $40\text{ }^\circ\text{C}$  suggests the micelle formation. The intermolecular interactions change from repulsive to attractive as the temperature goes up (see  $A_2$  in Fig. 11.17). These indicate that PNiPAM becomes hydrophobic by heating, and then the hydrophobic interaction between PNiPAM blocks induces the formation of micelles.

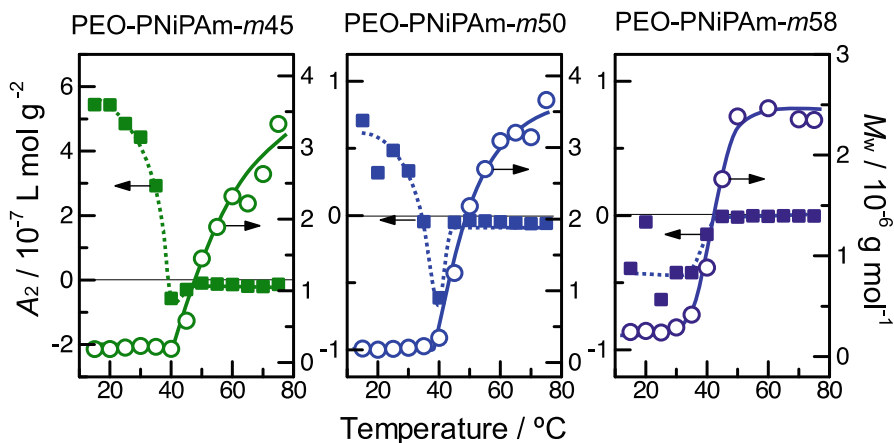


**Fig. 11.17** Temperature dependence of the apparent  $M_w$  (circles) and  $A_2$  (rectangles) for the 1.0 wt% aqueous solution of PEO-PNiPAm-*m*45, PNiPAm-*m*50, and PEO-PNiPAm-*m*58 measured by SLS. The values were recorded during the heating process. The original data of the figures are found in the reference [62]. The solid and dotted lines are drawn as guides to the eye

## 11.5 Conclusion

In this review, several examples have been introduced for shedding light on the molecular level solvation and hydration of amphiphilic polymers. Poly(*N,N*-diethylacrylamide), poly(*N*-isopropylacrylamide) (PNiPAm), and the alternating multiblock copolymer with poly(ethylene oxide) (PEO)-poly(propylene oxide) (PPO) and PEO-PNiPAm have been explained. The solvation of these polymers should be analyzed in terms of an explicit solvent molecule. We have to emphasize that the competition between solvation and intermolecular interactions is very important. The examples we showed here, however, give just an indirect evidence of how the molecular level interpretation of the solvation is important to understand the solution properties of amphiphilic polymers. To predict the solution property of functional polymers, the development of the explicit solvation model in theoretical and simulation studies for flexible, synthetic polymers is indispensable.

## References

1. Nakajima A, Hamada F, Hayashi S (2007) Unperturbed chain dimensions of polyethylene in theta solvents. *J Polym Sci Part C Polym Symp* 15:285–294. <https://doi.org/10.1002/polc.5070150120>
2. Sugiyama M, Nakamura Y, Norisuye T (2008) Dilute-solution properties of polystyrene polymacromonomer having side chains of over 100 monomeric units. *Polym J* 40:109–115. <https://doi.org/10.1295/polymj.PJ2007157>

3. Inagaki H (1966) The unperturbed dimensions of polypropylene and polyethylene. *J Phys Chem* 70:3420–3431. <https://doi.org/10.1021/j100883a009>
4. Doğan M, Kuntman A (2000) Study on conformational transition phenomena of poly(methyl methacrylate) in acetonitrile near theta conditions. *Polym Int* 49:1648–1652. [https://doi.org/10.1002/1097-0126\(200012\)49:12<1648::AID-PI578>3.0.CO;2-N](https://doi.org/10.1002/1097-0126(200012)49:12<1648::AID-PI578>3.0.CO;2-N)
5. Xia KQ, Franck C, Widom B (1992) Interfacial tensions of phase-separated polymer solutions. *J Chem Phys* 97:1446–1454. <https://doi.org/10.1063/1.463220>
6. Amu TC (1982) The unperturbed molecular dimensions of poly(ethylene oxide) in aqueous solutions from intrinsic viscosity measurements and the evaluation of the theta temperature. *Polymer (Guildf)* 23:1775–1779. [https://doi.org/10.1016/0032-3861\(82\)90121-5](https://doi.org/10.1016/0032-3861(82)90121-5)
7. Kubota K, Fujishige S, Ando I (1990) Solution properties of poly(N-isopropylacrylamide) in water. *Polym J* 22:15–20. <https://doi.org/10.1295/polymj.22.15>
8. Brandrup J, Immergut EH, Grulke EA et al (1999) *Polymer handbook*, 4th edn. Wiley, Boca Raton, FL
9. Flory PJ (1942) Thermodynamics of high polymer solutions. *J Chem Phys* 10:51–61. <https://doi.org/10.1063/1.1723621>
10. Huggins ML (1942) Some properties of solutions of long-chain compounds. *J Phys Chem* 46:151–158. <https://doi.org/10.1021/j150415a018>
11. Saeki S, Kuwahara N, Konno S, Kaneko M (1973) Upper and lower critical solution temperatures in polystyrene solutions. *Macromolecules* 6:246–250. <https://doi.org/10.1021/ma60032a020>
12. Konno S, Saeki S, Kuwahara N et al (1975) Upper and lower critical solution temperatures in polystyrene solutions. IV. Role of configurational heat capacity. *Macromolecules* 8:799–804. <https://doi.org/10.1021/ma60048a023>
13. Saeki S, Kuwahara N, Nakata M, Kaneko M (1976) Upper and lower critical solution temperatures in poly (ethylene glycol) solutions. *Polymer (Guildf)* 17:685–689. [https://doi.org/10.1016/0032-3861\(76\)90208-1](https://doi.org/10.1016/0032-3861(76)90208-1)
14. Kita R, Kircher G, Wiegand S (2004) Thermally induced sign change of Soret coefficient for dilute and semidilute solutions of poly(N-isopropylacrylamide) in ethanol. *J Chem Phys* 121:9140–9146. <https://doi.org/10.1063/1.1803535>
15. Ito D, Kubota K (1998) Anomalous scattering behavior of poly(N-n-propylacrylamide) in 2-propanol/water. *Chem Lett* 27:1283–1284. <https://doi.org/10.1246/cl.1998.1283>
16. Denisov VP, Halle B (1996) Protein hydration dynamics in aqueous solution. *Faraday Discuss* 103:227–244. <https://doi.org/10.1039/fd9960300227>
17. Zhang L, Wang L, Kao YT et al (2007) Mapping hydration dynamics around a protein surface. *Proc Natl Acad Sci USA* 104:18461–18466. <https://doi.org/10.1073/pnas.0707647104>
18. Uedaira H (1991) Hydration of biomolecules. *Seibutsu Butsuri* 31:155–160. <https://doi.org/10.2142/biophys.31.155>
19. Tanaka M, Mochizuki A (2010) Clarification of the blood compatibility mechanism by controlling the water structure at the blood-poly(meth)acrylate interface. *J Biomater Sci Polym Ed* 21:1849–1863
20. Ozaki Y, Wójcik MJ, Popp J, Katsumoto Y (2019) Spectral simulation for flexible molecules in solution with quantum chemical calculations. In: *Molecular spectroscopy*. Wiley, Boca Raton, FL, pp 253–277
21. Katsumoto Y, Tanaka T, Ozaki Y (2005) Molecular interpretation for the solvation of poly(acrylamide)s. I. Solvent-dependent changes in the C=O stretching band region of poly(N,N-dialkylacrylamide)s. *J Phys Chem B* 109:20690–20696. <https://doi.org/10.1021/jp052263r>
22. Ohno K, Okimura M, Akai N, Katsumoto Y (2005) The effect of cooperative hydrogen bonding on the OH stretching-band shift for water clusters studied by matrix-isolation infrared spectroscopy and density functional theory. *Phys Chem Chem Phys* 16:7. <https://doi.org/10.1039/b506641g>
23. Katsumoto Y, Tanaka T, Ozaki Y, Hosoi S (2009) Effects of dipole interaction and solvation on the C=O stretching band of N,N-dimethylacetamide in nonpolar solutions: infrared, isotropic

- and anisotropic Raman measurements. *Vib Spectrosc* 51:119–124. <https://doi.org/10.1016/j.vibspec.2008.11.009>
24. Miyazawa T, Shimanouchi T, Muzushima SI (1958) Normal vibrations of N-methylacetamide. *J Chem Phys* 29:611–616. <https://doi.org/10.1063/1.1744547>
  25. Katsumoto Y, Tanaka T, Sato H, Ozaki Y (2002) Conformational change of poly(N-isopropylacrylamide) during the coil-globule transition investigated by attenuated total reflection/infrared spectroscopy and density functional theory calculation. *J Phys Chem A* 106:3429–3435. <https://doi.org/10.1021/jp0124903>
  26. Coleman WM, Gordon BM (1988) Examinations of the matrix isolation FOURIER transform infrared spectra of organic compounds: part IX. *Appl Spectrosc* 42:1049–1056. <https://doi.org/10.1366/0003702894203895>
  27. Hashimoto C, Nagamoto A, Maruyama T et al (2013) Hydration states of poly(N-isopropylacrylamide) and poly(N,N-diethylacrylamide) and their monomer units in aqueous solutions with lower critical solution temperatures studied by infrared spectroscopy. *Macromolecules* 46:1041–1053. <https://doi.org/10.1021/ma302317m>
  28. Katsumoto Y, Tanaka T, Ihara K et al (2007) Contribution of intramolecular C=O...H-N hydrogen bonding to the solvent-induced reentrant phase separation of poly(N-isopropylacrylamide). *J Phys Chem B* 111:12730–12737. <https://doi.org/10.1021/jp0750452>
  29. Kamigaito M, Satoh K (2008) Stereoregulation in living radical polymerization. *Macromolecules* 41:269–276
  30. Ray B, Okamoto Y, Kamigaito M et al (2005) Effect of tacticity of poly(N-isopropylacrylamide) on the phase separation temperature of its aqueous solutions. *Polym J* 37:234–237. <https://doi.org/10.1295/polymj.37.234>
  31. Hirano T, Miki H, Seno M, Sato T (2005) Effect of polymerization conditions on the syndiotactic-specificity in radical polymerization of N-isopropylacrylamide and fractionation of the obtained polymer according to the stereoregularity. *Polymer (Guildf)* 46:5501–5505. <https://doi.org/10.1016/j.polymer.2005.05.043>
  32. Freitag R, Baltes T, Eggert M (1994) A comparison of thermoreactive water-soluble poly-N,N-diethylacrylamide prepared by anionic and by group transfer polymerization. *J Polym Sci Part A Polym Chem* 32:3019–3030. <https://doi.org/10.1002/pola.1994.080321603>
  33. Kobayashi M, Ishizone T, Nakahama S (2000) Synthesis of highly isotactic poly(N,N-diethylacrylamide) by anionic polymerization with grignard reagents and diethylzinc. *J Polym Sci Part A Polym Chem* 38:4677–4685. [https://doi.org/10.1002/1099-0518\(200012\)38:1+<4677::aid-pola70>3.3.co;2-r](https://doi.org/10.1002/1099-0518(200012)38:1+<4677::aid-pola70>3.3.co;2-r)
  34. Katsumoto Y, Kubosaki N (2008) Tacticity effects on the phase diagram for poly(N-Isopropylacrylamide) in water. *Macromolecules* 41:5955–5956. <https://doi.org/10.1021/ma800881r>
  35. Katsumoto Y, Etoh Y, Shimoda N (2010) Phase diagrams of stereocontrolled poly(N,N-diethylacrylamide) in water. *Macromolecules* 43(6):3120–3121. <https://doi.org/10.1021/ma902673z>
  36. Tong Z, Zeng F, Zheng X, Sato T (1999) Inverse molecular weight dependence of cloud points for aqueous poly(N-isopropylacrylamide) solutions. *Macromolecules* 32:4488–4490. <https://doi.org/10.1021/ma990062d>
  37. Kawaguchi T, Kobayashi K, Osa M, Yoshizaki T (2009) Is a cloud-point curve in aqueous poly(N-isopropylacrylamide) solution binodal? *J Phys Chem B* 113:5440–5447. <https://doi.org/10.1021/jp9005795>
  38. Hamamura K, Watanabe K, Sanada Y et al (2019) Relationship between the phase diagram and hysteresis in demixing and remixing for atactic and meso-rich poly(N-isopropylacrylamide)s in water. *Polymer (Guildf)* 161:92–100. <https://doi.org/10.1016/j.polymer.2018.12.001>
  39. Okada Y, Tanaka F (2005) Cooperative hydration, chain collapse, and flat LCST behavior in aqueous poly(N-isopropylacrylamide) solutions. *Macromolecules* 38:4465–4471. <https://doi.org/10.1021/ma0502497>

40. Katsumoto Y, Kubosaki N, Miyata T (2010) Molecular approach to understand the tacticity effects on the hydrophilicity of poly(*N*-isopropylacrylamide): solubility of dimer model compounds in water. *J Phys Chem B* 114:13312–13318. <https://doi.org/10.1021/jp107442h>
41. Maeda Y, Nakamura T, Ikeda I (2002) Change in solvation of poly(*N,N*-diethylacrylamide) during phase transition in aqueous solutions as observed by IR spectroscopy. *Macromolecules* 35:10172–10177. <https://doi.org/10.1021/ma020945w>
42. Wang X, Qiu X, Wu C (1998) Comparison of the coil-to-globule and the globule-to-coil transitions of a single poly(*N*-isopropylacrylamide) homopolymer chain in water. *Macromolecules* 31:2972–2976. <https://doi.org/10.1021/ma971873p>
43. Cheng H, Shen L, Wu C (2006) LLS and FTIR studies on the hysteresis in association and dissociation of poly(*N*-isopropylacrylamide) chains in water. *Macromolecules* 39:2325–2329. <https://doi.org/10.1021/ma052561m>
44. Lu Y, Zhou K, Ding Y et al (2010) Origin of hysteresis observed in association and dissociation of polymer chains in water. *Phys Chem Chem Phys* 12:3188. <https://doi.org/10.1039/b918969f>
45. Li PF, Wang W, Xie R et al (2009) Lower critical solution temperatures of thermo-responsive poly(*N*-isopropylacrylamide) copolymers with racemate or single enantiomer groups. *Polym Int* 58:202–208. <https://doi.org/10.1002/pi.2517>
46. Shen Z, Terao K, Maki Y et al (2006) Synthesis and phase behavior of aqueous poly(*N*-isopropylacrylamide-co-acrylamide), poly(*N*-isopropylacrylamide-co-*N,N*-dimethylacrylamide) and poly(*N*-isopropylacrylamide-co-2-hydroxyethyl methacrylate). *Colloid Polym Sci* 284:1001–1007. <https://doi.org/10.1007/s00396-005-1442-y>
47. Keerl M, Richtering W (2007) Synergistic depression of volume phase transition temperature in copolymer microgels. *Colloid Polym Sci* 285:471–474. <https://doi.org/10.1007/s00396-006-1605-5>
48. Scherzinger C, Lindner P, Keerl M, Richtering W (2010) Cononsolvency of poly(*N,N*-diethylacrylamide) (PDEAAM) and poly(*N*-isopropylacrylamide) (PNIPAM) based microgels in water/methanol mixtures: copolymer vs core-shell microgel. *Macromolecules* 43:6829–6833. <https://doi.org/10.1021/ma100422e>
49. Maeda Y, Yamabe M (2009) A unique phase behavior of random copolymer of *N*-isopropylacrylamide and *N,N*-diethylacrylamide in water. *Polymer (Guildf)* 50:519–523. <https://doi.org/10.1016/j.polymer.2008.11.032>
50. Lutz J-F, Ouchi M, Liu DR, Sawamoto M (2013) Sequence-controlled polymers. *Science* 341:1238149. <https://doi.org/10.1126/science.1238149>
51. Anderson BC, Cox SM, Bloom PD et al (2003) Synthesis and characterization of diblock and gel-forming pentablock copolymers of tertiary amine methacrylates, poly(ethylene glycol), and poly(propylene glycol). *Macromolecules* 36:1670–1676. <https://doi.org/10.1021/ma0211481>
52. Determan MD, Cox JP, Seifert S et al (2005) Synthesis and characterization of temperature and pH-responsive pentablock copolymers. *Polymer (Guildf)* 46:6933–6946. <https://doi.org/10.1016/j.polymer.2005.05.138>
53. Peleshanko S, Anderson KD, Goodman M et al (2007) Thermoresponsive reversible behavior of multistimuli pluronic-based pentablock copolymer at the air-water interface. *Langmuir* 23:25–30. <https://doi.org/10.1021/la061547f>
54. Lu Y, Chen T, Mei A et al (2013) Solution behaviors and microstructures of PNIPAm-P123-PNIPAM pentablock terpolymers in dilute and concentrated aqueous solutions. *Phys Chem Chem Phys* 15:8276–8286. <https://doi.org/10.1039/c3cp50376c>
55. Holtzer A, Emerson MF (1969) On the utility of the concept of water structure in the rationalization of the properties of aqueous solutions of proteins and small molecules. *J Phys Chem* 73:26–33. <https://doi.org/10.1021/j100721a005>
56. Moriyama Y, Watanabe E, Kobayashi K et al (2008) Secondary structural change of bovine serum albumin in thermal denaturation up to 130 °C and protective effect of sodium dodecyl sulfate on the change. *J Phys Chem B* 112:16585–16589. <https://doi.org/10.1021/jp8067624>
57. Rikiyama K, Horiuchi T, Koga N et al (2018) Micellization of poly(ethylene oxide)-poly(propylene oxide) alternating multiblock copolymers in water. *Polymer (Guildf)* 156:102–110. <https://doi.org/10.1016/J.POLYMER.2018.09.047>



58. Alexandridis P, Holzwarth JF, Hatton TA (1994) Micellization of poly(ethylene oxide)-poly(propylene oxide)-poly(ethylene oxide) triblock copolymers in aqueous solutions: thermodynamics of copolymer association. *Macromolecules* 27:2414–2425. <https://doi.org/10.1021/ma00087a009>
59. Horiuchi T, Sakai T, Sanada Y et al (2017) Association behavior of poly(ethylene oxide)–poly(propylene oxide) alternating multiblock copolymers in water toward thermally induced phase separation. *Langmuir* 33:14649–14656. <https://doi.org/10.1021/acs.langmuir.7b02810>
60. Moghimi SM, Hunter AC (2000) Poloxamers and poloxamines in nanoparticle engineering and experimental medicine. *Trends Biotechnol* 18:412–420
61. Alexandridis P, Alan Hatton T (1995) Poly(ethylene oxide)poly(propylene oxide)poly(ethylene oxide) block copolymer surfactants in aqueous solutions and at interfaces: thermodynamics, structure, dynamics, and modeling. *Colloids Surfaces A Physicochem Eng Asp* 96:1–46. [https://doi.org/10.1016/0927-7757\(94\)03028-X](https://doi.org/10.1016/0927-7757(94)03028-X)
62. Rikiyama K, Sanada Y, Watanabe K et al (2019) Unimer structure and micellization of poly(ethylene oxide)-stereocontrolled poly(N-isopropylacrylamide) alternating multiblock copolymers in aqueous solution. *Macromolecules* 52:7188–7196. <https://doi.org/10.1021/acs.macromol.9b01172>